PCCP

Cite this: *Phys. Chem. Chem. Phys.*, 2011, **13**, 19741–19748

www.rsc.org/pccp

PAPER

Heat capacity and glass transition in P_2O_5–H_2O solutions: support for Mishima's conjecture on solvent water at low temperature

Horacio R. Corti,*[ab] Federico J. Nores-Pondal†[a] and C. Austen Angell[c]

Received 3rd July 2011, Accepted 19th August 2011
DOI: 10.1039/c1cp22185j

The P_2O_5–water system has the widest range of continuously glass-forming compositions known for any glassformer + water binary system. Despite the great range of structures explored by the glasses and liquids in this system, the glass transition temperature (T_g) itself varies in a simple monotonic fashion. However the values of T_g reported in the literature show wide disagreement, linked to the different methods of measurement employed. In this work we use differential scanning calorimetry (DSC) to obtain both T_g itself and the jump in heat capacity that occurs as the metastable equilibrium of the supercooled liquid relieves the non-ergodic glassy state. Our study covers the molar ratio range of H_2O/P_2O_5 from 1.5 to 14 (corresponding to the mass fraction of P_2O_5 between 0.36 and 0.84), which includes the compositions corresponding to pyrophosphoric acid ($H_4P_2O_7$) and orthophosphoric acid (H_3PO_4). The theoretical model of Couchman and Karasz predicts very well the glass transition temperatures of the P_2O_5–H_2O system over the whole composition range if the relatively large heat capacity change associated with water in aqueous solutions at the glass transition temperature is adopted, instead of the vanishingly small value observed for vapor deposited or hyperquenched pure water. Therefore, solvent water in this ambient pressure P_2O_5–H_2O system behaves like a different liquid, more closely resembling a high-density liquid (HDL) polyamorph, as suggested by Mishima for electrolytes at high pressures.

1. Introduction

Water is nature's most ubiquitous solvent. While water acting as a solute dissolves in many low melting liquid salts to form almost ideal solutions, water as a solvent can be the seat of much complexity. Salts and other dissociating solvents form very complicated solutions in water, and their description becomes increasingly complex as the temperature under consideration is decreased. This seems to be related to the particularly anomalous character of water itself, which is the source of much current discussion and controversy. A variety of anomalies, in both thermodynamic and dynamic properties of pure water, have been given a consistent interpretation in terms of a hidden critical point lying just below the homogeneous nucleation limit to the supercooled liquid state. These anomalies persist, with decreasing magnitude, until the first eutectic involving crystalline ice has been reached. Indeed it is only in the solutions that the actual phase separation (which is hypothetical for pure water because of the pre-emptive ice formation) can be seen. Mishima, in particular, has documented the first order transition character of some of the phase changes observed very close to the glass temperature in the LiCl–water system,[1–3] where the crystallization is sufficiently separated in the time scale as not to interfere with the observations. Indeed it is likely that such first order phase separations will be observable in all of the systems that show an arrest in the T_g *vs.* composition plot, as pure water limit is approached (see Fig. 3 and 5 of ref. 4). Mishima has suggested, on the basis of these and related observations that, near T_g, water in these concentrated solutions mimics the properties of HDL rather than the LDL liquid polyamorph.[3]

In the search for understanding of this complex domain, where the structure has been described as having "wormhole" character[4] (now seen as anticipating the phase separation), it is helpful to refine our description of solution behavior in the *less* complex domains of composition. Indeed, in the very concentrated solution domain, a number of systems seem to behave with great simplicity. For instance, the calcium nitrate–water system can be explored over a range of compositions in which the water : salt

[a] *Departamento de Física de la Materia Condensada, Centro Atómico Constituyentes, Comisión Nacional de Energía Atómica, San Martín (1650), Buenos Aires, Argentina. E-mail: hrcorti@cnea.gov.ar; Fax: +54 11 6772 7886; Tel: +54 11 6772 7174*
[b] *Instituto de Química Física de los Materiales, Ambiente y Energía (INQUIMAE), Facultad de Ciencias Exactas y Naturales, Universidad de Buenos Aires, Buenos Aires (1428), Argentina*
[c] *Department of Chemistry and Biochemistry, Arizona State University, Tempe, Arizona 85287, USA*
† Current address: Laboratory of Components for Fuel Cells, and Electrolysers, and of Modeling (LCPEM), Commission for Atomic and Alternative Energies of France, 38054 Grenoble Cedex 9, France.

ratio varies from 2.5 to 20. Over this range the temperature T_g, at which viscosity reaches a value where flow effectively ceases and a glass is formed, changes in a simple linear fashion.[4] The glass forms because the liquid response time to shear perturbations changes extremely rapidly with temperature and becomes of the order of minutes at T_g.

Even more impressive is the behavior observed in the system P_2O_5 + water. In this system solutions that can be vitrified are available all the way to the pure oxide itself. In this important system, which provides fuel cell electrolyte compositions for elevated temperature technology, the glass transition temperatures will be shown to vary in a monotonic manner that can be well accounted for by a popular equation developed for polymer–solvent mixtures by Couchman and Karasz,[5] based on the Adam–Gibbs entropy theory of the glass transition.[6] For this equation to account for all the data, however, it will be found necessary to adopt a value of heat capacity jump at T_g which is appropriate for the limiting glass-forming solution at the water-rich end of the glassforming range, rather than the value for pure water. In this respect the P_2O_5–water system provides useful input for the phenomenological description of water and its solutions in the complex low water concentration domain, as we will describe in the discussion section of this paper.

The paper is organized as follows. First we review the nature and importance of the pure component phosphorus pentoxide (P_2O_5), which is one of the important components of the optical glass industry and is of special importance to the giant laser project because of its unusual transparency in the near UV frequency range. Then we consider the series of compounds formed by P_2O_5–water combinations, of which orthophosphoric acid (H_3PO_4) is the most important. Finally we will concentrate on the glass transition phenomenology, provide a quantitative description of the composition dependence of T_g over the major part of its occurrence in this system, and discuss the implications for solution structure in the lower concentration, non-glassforming domain of aqueous solutions.

2. The glass transition of the P_2O_5–water system

P_2O_5, one of the three primary "glass former" oxides (along with SiO_2 and B_2O_3), is used as a major component,[7] or as a dopant,[8] in the preparation of many glasses. Mixtures of P_2O_5 with 3d-transition metal oxides have also received considerable attention because of their semiconducting and optical properties and potential applications.[9,10] For this reason the thermal properties of its mixtures with metal oxides are well known.[11,12]

Combined with water, P_2O_5 forms a series of phosphoric acids, orthophosphoric acid (H_3PO_4) being the most important in chemical applications, and serving also as a protonic conductor in developing fuel cells. In this last application it can be used pure (phosphoric acid fuel cells) or soaked in a polymeric matrix, such as polybenzimidazole,[13] in the case of proton exchange membranes fuel cells (PEMFC) with hydrogen or methanol feeds.

In spite of their practical relevance, the glass transition temperatures, T_g, of P_2O_5 and its mixtures with water remain very uncertain. Thus, T_g for pure P_2O_5 remains elusive, probably because of its polymorphism[8,14,15] and its sensitivity to traces of water that are extremely difficult to remove. The first reported glass transition temperature (T_g = 535 K) of pure P_2O_5 was indirectly obtained by Sakka and McKenzie,[16] by extrapolating viscosity data obtained over a higher temperature range.[17] Martin and Angell[18] employed, for the first time, the differential scanning calorimetry (DSC) technique for direct measurement, finding T_g = (590 ± 2) K. Later, Hudgens and Martin[19] studied anhydrous P_2O_5 samples carefully prepared by sublimation of the compound in a dry atmosphere and obtained T_g = 653 K, clearly indicating that the T_g value is strongly affected even by trace quantities of water.

Recently, Sidebottom and Changstrom[20] measured the viscoelastic relaxation in molten P_2O_5, using photon correlation spectroscopy, from 850 °C to near the glass transition temperature, and obtained T_g = (692 ± 10) K by extrapolation to an average relaxation time of 100 s. These authors also confirmed that, as suggested by Martin and Angell,[18] P_2O_5 behaves as a strong glass-forming liquid, with a fragility index similar to that reported for SiO_2 and GeO_2.[21]

On the other hand, Kobeko *et al.*[22] reported T_g = 152 K for H_3PO_4, determined from the temperature dependence of the electrical conductivity. There were no other measurements of the glass transition temperature of the P_2O_5–H_2O system until Ellis[23] measured T_g by resorting to the change of the NMR linewidth of the P_2O_5–H_2O mixtures at the glass–liquid transition. The composition of the system, expressed in terms of the water/P_2O_5 mole ratio, R, covered the range $1.17 < R < 3.95$ and the measured T_g of the P_2O_5–H_2O mixtures lay on a straight line (T_g = 281.1–17.28 R) when represented as a function of R, including the metaphosphoric acid composition (HPO_3), with R = 1, measured by Eisenberg *et al.*[24] Thus, Ellis predicted T_g = (229 ± 2) K for pure orthophosphoric acid (R = 3), a value much higher than that determined by Kobeko *et al.*[22] and enshrined in the literature.[25]

Aihara *et al.*[26] performed a detailed study on the ion conduction mechanisms of anhydrous and hydrated phosphoric acids, and reported T_g values, obtained by DSC, for phosphoric acid concentrations in the range $1.50 < R < 6.63$. The T_g values measured by these authors were much lower than those reported by Ellis[23] (T_g = (200 ± 1) K for orthophosphoric acid).

In this work, we determine T_g and the heat capacity change at T_g for the P_2O_5–H_2O system, over the range of composition from R = 1.5 to R = 13.9, using DSC as the most direct method, in order to obtain a reliable value for H_3PO_4, and to rationalize the concentration dependence of T_g in terms of available glass transition models for mixtures.

3. Experimental

3.1 Materials

The phosphoric acid samples below 85 wt% were prepared by dilution of phosphoric acid 85% (Merck, grade Ph Eur, BP, NF, E 338) using ultrapure water (Milli-Q). The samples with concentrations above 85 wt% were prepared by hydration of P_2O_5 (Baker, ACS spec.), controlled by weighing, or by addition of water to polyphosphoric acid (Aldrich, reagent grade 115% H_3PO_4) corresponding to R = 1.58 (implies

Table 1 Glass transition temperature and heat capacity changes at T_g of P_2O_5–H_2O mixtures as a function of composition

w_2	x_2	R	T_g onset/K	T_g midpoint/K	$\Delta C_p{}^a$ /J K^{-1} mol^{-1}
0.361	0.067	13.93	151.0	153.1	34.2
0.433	0.088	10.31	154.2	155.4	38.5
0.451	0.094	9.60	156.3	157.7	38.6
0.498	0.112	7.96	161.3	161.9	32.5
0.529	0.125	7.02	164.7	165.6	32.1
0.559	0.138	6.23	169.3	170.4	
0.587	0.153	5.54	171.0	172.2	41.4
0.620	0.171	4.84	177.2	179.0	41.6
			176.5	177.6	43.5
			176.4	177.5	42.2
0.664	0.200	4.00	183.0	184.2	38.9
0.688	0.219	3.57	186.7	187.9	38.3
0.724	0.250	3.00	188.7	190.2	40.2
			189.3	190.7	38.2
			192.9	199.0	35.7
0.833	0.387	1.58	231.4	233.6	33.7
0.839	0.398	1.51	231.2	233.0	38.7

[a] Per total moles (H_2O + P_2O_5), at each composition.

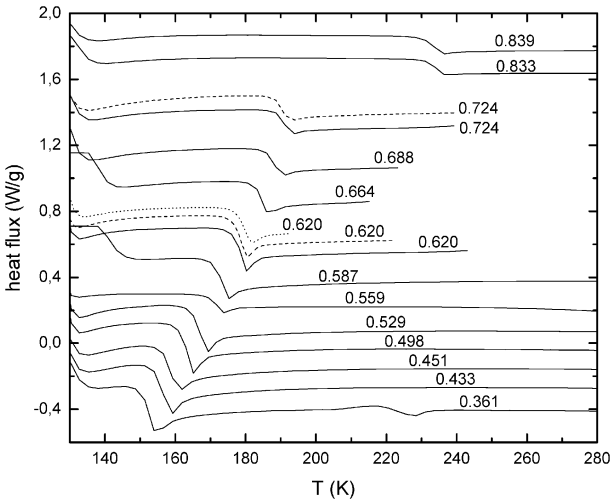

Fig. 1 DSC scans for water–P_2O_5 mixtures obtained at a rate of 10 K min^{-1}. The mass fraction of P_2O_5 (w_2) is indicated on each curve (H_3PO_4 stoichiometry has w_2 = 0.724). Dotted and dashed lines at w_2 = 0.620 and 0.724 correspond to duplicate and triplicate runs.

~0.7% uncertainty in composition). No attempts were made to determine the glass transition temperature of pure P_2O_5 in view of its extreme sensitivity to traces of water.

The concentrations of the samples, summarized in Table 1, are expressed as a weight fraction of P_2O_5 (w_2), which is related to R, the mole ratio of water to P_2O_5, by the expression $1/w2 = (1 + R/7.886)$, where 7.886 is the molar weight ratio $M_{P_2O_5}/M_{H_2O}$. The compositions of the mixtures, expressed as mole fractions of P_2O_5, $x_2 = (R + 1)^{-1}$, are also reported in Table 1. The weight fraction of H_3PO_4, denoted by w_2^*., is also used in this work to analyze the equations for the glass transition temperature of the binary systems. For the pure orthophosphoric acid (R = 3), w_2^*. = 1, which corresponds to w_2 = 0.724.

3.2 Thermophysical properties

The glass transition temperatures were determined by differential scanning calorimetry (DSC) using a Mettler 822 and STARe Thermal Analysis System version 6.1 software (Mettler Toledo AG, Switzerland). The instrument was calibrated using standard compounds (indium, zinc and lead in the high temperature range, and *n*-heptane and *n*-octane in the low temperature range). The scans were performed from −145 to 25 °C and onset and midpoint T_g to ±0.5 K were obtained, using the DSC software, from the curves of heat-flow *vs.* temperature. Typical differences between onset and midpoint values of T_g were 1–2 K. The heat capacities at the glass transition were calculated from the slope of the heat flow *vs.* time at T_g and the sample mass.

All measurements were performed with sample mass in the range 8–20 mg, at a scanning rate of 10 K min^{-1} using hermetically sealed gold plated stainless steel pans of 40 μL inner volume (Mettler) and an empty pan was used as a reference.

4. Results

4.1 Glass transition temperatures and heat capacity changes

Fig. 1 shows the DSC scans for the samples studied in this work. It is seen that T_g shifts systematically to higher temperatures with increasing P_2O_5 concentration (decreasing R). The onset and midpoint glass transition temperatures, along with the corresponding changes of heat capacity per mole of solution at the glass transition, are summarized in Table 1.

Our study extends over a wider concentration range (down to w_2 = 0.361, R = 13.93) than those previously reported, as shown in the phase diagram, Fig. 2, which includes the results obtained by other authors.[26,22–24]

It is observed that previous data obtained by DSC[26] agree quite reasonably with those measured in this work, while the T_g values for aqueous mixtures determined by NMR[23] are higher than those determined by DSC for P_2O_5 weight fractions w_2 < 0.85. The physical reason for NMR giving a higher temperature than the DSC study, or any study conducted on the time scale of minutes (by which the T_g is usually defined calorimetrically) is that the typical NMR frequency is in the MHz range so, just as happens in the scan in a dielectric relaxation experiment, the system will "break ergodicity" at the temperature where the relaxation time of the liquid is the inverse of the probe frequency. Also, because the system falls out of equilibrium with respect to the perturbing stress at a much higher temperature, it must take a larger temperature range to pass through the "glass transformation zone" (which is about two decades wide), and so the difference between midpoint and onset temperature must spread out, as observed in the reported plot of NMR linewidth against temperature,[23] where this difference is around 45 K. In summary, the measurement of the NMR linewidth temperature dependence is simply not a suitable technique for T_g determination.

The mean value of the onset glass transition temperature of the orthophosphoric acid reported in Table 1 is T_g = 190.3 K.

The more dilute solutions (w_2 < 0.450) measured in this work correspond to P_2O_5–H_2O mixtures having more water than the eutectic composition. The onset of ice formation is observed in Fig. 1 for the thermogram corresponding to the solution with w_2 = 0.361, and this determines the low concentration limit of our study. On the other hand, the more

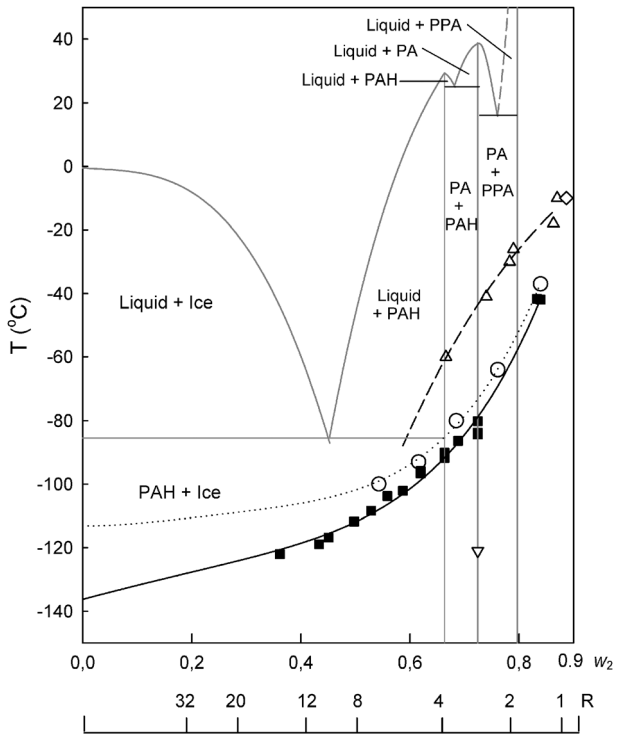

Fig. 2 Supplemented phase diagram of the system phosphoric acid–water, showing the coexistence of liquid–solid and solid–solid phases (PA: orthophosphoric acid (H_3PO_4); PAH: orthophosphoric acid hemi-hydrate ($H_3PO_4{\cdot}\frac{1}{2}H_2O$); PPA: pyrophosphoric acid ($H_4P_2O_7$), adapted from the known phase diagram,[25] and the glass transition temperature (onset) from: (■) this work, (○) ref. 26; (△) ref. 23; (◊) ref. 24; (▽) ref. 22. Both composition scales, w_2 and R, were used. The solid line is the best fit of our data extended up to the glass transition of pure water (−137 °C); the dotted line represents the fit of the data by Aihara *et al.*;[26] the dashed line is the extrapolation of the data by Ellis.[23]

concentrated solutions extend to the pure orthophosphoric acid and into the region where P_2O_5 and pyrophosphoric acid ($H_4P_2O_7$) coexist.[27]

From the values reported in Table 1, it can be concluded that ΔC_p per mol of mixture (H_2O + P_2O_5) at the glass transition is relatively independent of the composition up to $x_2 \approx 0.4$, the mean value being (37.7 ± 2.5) J K^{-1} mol^{-1}. The heat capacity change must decrease at some composition with $x_2 > 0.4$ and must extrapolate in the limit $x_2 = 1$ to the value measured by Martin and Angell[18] for pure P_2O_5 in the glass transition region, $\Delta C_{p2} = 2.1$ J K^{-1} mol^{-1}.

The extrapolation to pure water is performed by plotting (see Fig. 3) the ΔC_p per mol of water at the glass transition temperature as a function of x_2. The scatter in the data is too large to decide whether a linear or a quadratic fit is better, but in any case the extrapolated values are in the range 31–35 J K^{-1} mol^{-1}, in good agreement with the values found for aqueous solutions of hydrogen bonding solutes, like H_2O_2 and N_2H_4 (at $x_2 \approx 0.37$).[28]

The experimental difficulties in identifying the glass transition for pure water, and particularly in determining the associated heat capacity change, are well known, but it is now accepted that ΔC_p for pure water is much lower than the values

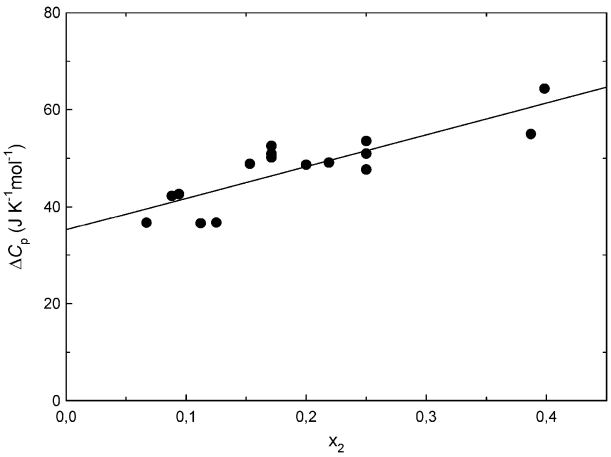

Fig. 3 Change of the heat capacity per mol of water of P_2O_5–H_2O mixtures, at the glass transition, as a function of the composition. The solid line shows the linear fit of the data.

obtained by extrapolations from aqueous solutions.[29] We will discuss this point in detail in Section 5.

4.2 Empirical and theoretical models of T_g for binary mixtures

In order to describe the concentration dependence of the glass transition temperature in the range of w_2 between 0.54 and 0.84 in the present system, Aihara *et al.*[26] proposed the empirical expression,

$$T_g = T_g^0 + \alpha \exp(\beta c) \quad (1)$$

where α = (0.76 ± 0.07) K, β = 0.040 ± 0.001, c is the concentration (in wt%), and T_g^0 = (159.7 ± 0.7) K, obtained from linear regression. T_g^0 is referred as the glass transition of pure water[26] but, according to eqn (1), for pure water $T_g = T_g^0 + \alpha$. In summary, eqn (1) has three empirical parameters with no physical meaning and certainly is not adequate to describe the dependence on composition of the glass transition temperature of the binary P_2O_5–H_2O mixtures. Accordingly, it seems reasonable to explore the known theoretical solution models to predict the glass transition temperature from the known thermophysical properties of the pure components at their glass transitions. There are several to consider.

The Gordon and Taylor (GT) model, based on the free volume theory of liquids,[30] was originally developed to predict the glass transition temperature of polymer blends.[31] It allows the calculation of the T_g of the mixture from the T_g values of the pure components,

$$T_g = \frac{w_2 T_{g2} + w_1 k_{GT} T_{g1}}{w_2 + w_1 k_{GT}} \quad (2)$$

where w_1 and w_2 are the weight fraction of water and P_2O_5, respectively, T_{g1} and T_{g2} are the glass transition temperatures of water and P_2O_5, respectively, and the coefficient $k_{GT} = \rho_2 T_{g2}/\rho_1 T_{g1}$ can be calculated from the densities of the pure components at T_g. In this particular case the volumetric data for the P_2O_5–H_2O mixtures on the glass transition curve are not available to test the model.

The second model, due to Couchman and Karasz (CK),[5] treats the glass transition as, ideally, an Ehrenfest second order

transition in which the enthalpy, entropy and volume of the mixture are continuous at T_g, and the heat capacity change at the glass transition, $\Delta C_{pi} = C_{pi}(liq) - C_{pi}(glass)$, is assumed to be independent of the temperature. Goldstein[32] criticized this approach, arguing that, for the excess entropy of mixing of the glass, the pure components entropies should not all be of the glass but those of the actual states at the condition of interest. Couchman[33] discussed the alternative definition of entropy of mixing proposed by Goldstein and showed that it led to inconsistencies. Although an alternative approach taking into account the effect of the entropy of mixing on the glass has recently been proposed,[34] the CK model is commonly used for prediction of glass transition in aqueous systems.[35]

A modification of the CK model, due to Ten Brinkle *et al.*,[36] considers that the heat capacity changes are proportional to the temperature, leading to the following expression

$$T_g = \frac{w_2 T_{g2} + w_1 k_{CK} T_{g1}}{w_2 + w_1 k_{CK}} \quad (3)$$

which is equivalent to eqn (3), except that k_{CK} is given in terms of the corresponding heat capacity change of the pure components at the glass transition:

$$k_{CK} = \frac{\Delta C_{p1}}{\Delta C_{p2}} \quad (4)$$

Eqn (2) and (3), are usually considered as empirical equations with the coefficients k_{GT} or k_{CK} as adjustable parameters. Thus, both equations can be expressed in the linear form,

$$\frac{T_g - T_{g2}}{T_g - T_{g1}} = k\left(1 - \frac{1}{w_2}\right) \quad (5)$$

which is more suitable for linear regression analysis.

Thus, using glass transition temperature of pure water, $T_{g1} = (136 \pm 1)$ K, reported for amorphous solid water[37–39] and hyperquenched water,[39–44] and the T_{g2} values for pure P_2O_5 obtained from direct DSC measurements (more reliable than the extrapolated ones) by Martin and Angell[18] ($T_{g2} = 590$ K) and by Hudgens and Martin[19] ($T_{g2} = 653$ K), we calculated from eqn (5) the best fit k parameters reported in Table 2. Also reported is the k parameter obtained on the restricted composition range limited by orthophosphoric acid ($w_2 = 0.724$, $R = 3$). The three sets of parameters (T_{g2} and k) describe, within the experimental error, the T_g *vs.* w_2 curve (Fig. 2) on the measured composition range ($0.361 < w_2 < 0.839$), indicating that, at least for $w_2 < 0.839$, the large differences in the reported T_{g2} values have a negligible impact on the fit of the T_g of P_2O_5–H_2O mixtures.

4.3 Test of the CK model for the P_2O_5–H_2O system

In order to test the validity of the CK model for describing T_g of the P_2O_5–H_2O mixtures, k_{GT} will be calculated from eqn (3) and (4), using the thermophysical information available for the pure components. The above quoted values $T_{g1} = (136 \pm 1)$ K and T_{g2} (590 K and 653 K) were used in this case in eqn (3), but the coefficient k_{CK} was calculated from the ΔC_{p1} and ΔC_{p2} values for the pure components. As mentioned in Section 4.1, for pure P_2O_5, $\Delta C_{p2} = 2.1$ J K^{-1} mol^{-1} is the only value reported in the literature.[18]

Table 2 Parameters of eqn (5) for the P_2O_5–H_2O and H_3PO_4–H_2O systems

System	T_{g1}/K	T_{g2}/K	k	Range
P_2O_5–H_2O	136	590	16.7	$0 < w_2 < 1$
P_2O_5–H_2O	136	653	19.0	$0 < w_2 < 1$
H_3PO_4–H_2O	136	190.3	2.76	$0 < w_2 < 0.724$ $(0 < w_2^* < 1)$

Different results have been reported for ΔC_{p1} depending on the way the vitrification of pure water is performed. Sugisaki *et al.*[37] measured $\Delta C_{p1} = 35$ J K^{-1} mol^{-1} for vapor-deposited amorphous water, while MacFarlane and Angell[45] did not detect any C_p increase within the instrument sensitivity (0.4 J K^{-1} mol^{-1}) when the vapour deposition was made directly into a DSC sample pan. Hallbrucker *et al.*,[38] using special annealing techniques to enhance the relaxation strength, determined $\Delta C_{p1} = 1.6$ J K^{-1} mol^{-1} for hyperquenched glassy water. The most recent assessment[29] of the heat capacity change for samples of hyperquenched pure water is $\Delta C_{p1} = 0.70$ J K^{-1} mol^{-1} at $T_{g1} = 140$ K.

On the other hand, measurements of ΔC_p at T_g made over a range of compositions of several glass-forming aqueous salt systems[46] yielded $\Delta C_{p1} = (20.0 \pm 0.9)$ J K^{-1} mol^{-1}, by extrapolation to pure water, while even larger values, 35 J K^{-1} mol^{-1}, were observed for the hydrogen-bonded molecular solutions H_2O–H_2O_2 and H_2O–N_2H_4,[28] as mentioned in Section 4.1. A "fragile-to-strong" liquid transition in the "no-man's land" with dramatic C_p decrease seems the most likely explanation for these discrepancies,[47,48] though a hidden glass transition of larger magnitude within the no-man's land has also been suggested on the basis of hyperquenched inorganic glass studies.[49]

The value $\Delta C_{p1} = 35$ J K^{-1} mol^{-1} has also proved the most appropriate for calculations of T_g of the (hydrogen-bonded) trehalose and sucrose aqueous solutions using the CK equation,[35] which is consistent with data from the H_2O_2 and N_2H_4 aqueous solutions. It is then not surprising to find the extrapolated value of ΔC_{p1} lying in the range 31–35 J K^{-1} mol^{-1} (see Fig. 3), obtained in this work for the mixed ionic/hydrogen bonded P_2O_5–H_2O mixtures. Using these ΔC_{p1} values the calculated k_{CK} ranged between 14.8 and 17.6, in excellent agreement with the fitted data reported in Table 2, particularly when the $T_{g2} = 590$ K[18] is used for P_2O_5.

Fig. 4 shows that both values of k_{CK} render essentially the same fit in the composition region studied in this work, except for the region close to pure P_2O_5 ($0.9 < w_2 < 1$) where no measurements were performed in this work.

The inset of Fig. 4 illustrates the results in the region of concentration up to pure H_3PO_4 (*i.e.* in the subsystem H_2O–H_3PO_4) and the best fit with eqn (5) using $T_{g2} = 190.3$ K, the mean value determined in this work, and expressing the concentration as a weight fraction of H_3PO_4 (w_2^*). In this case the best fit value (see Table 2) is $k_{CK} = 2.76$, indicating that the plasticizing effect of water on H_3PO_4 is much lower than that on P_2O_5.

5. Discussion

The very good agreement between the calculated and measured k_{CK} is unlikely to be fortuitous. The implication is

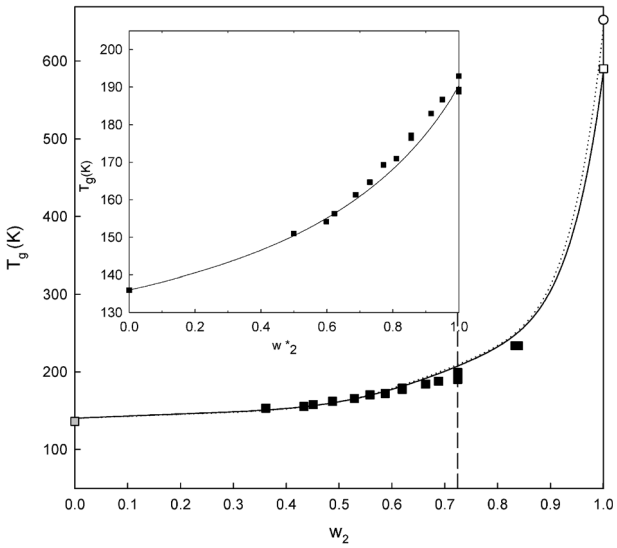

Fig. 4 The glass transition temperature of P_2O_5–H_2O mixtures as a function of the weight fractions of P_2O_5. The solid and dotted lines correspond to the fits using eqn (5) with the T_{g2} values reported in ref. 18 (□) and 19 (○), respectively. The dashed line represents the composition corresponding to H_3PO_4. Inset: glass transition temperature of H_3PO_4–H_2O mixtures as a function of the weight fraction of H_3PO_4. The solid line corresponds to the best fit using eqn (5) and the parameters described in the text.

that over wide ranges of solution composition, the degrees of freedom explored by the water molecules near the solution glass transitions are essentially the same in all these systems. But they are clearly not the same as those explored near T_g for LDL water, where the jump in heat capacity at T_g is nearly 20 times smaller.

The existence of other forms of amorphous water is now well known[50–52] though the high density forms known as high density amorphous (HDA) and very high density amorphous (VHDA) are thought by many to be different density states of the same phase.[52]

In Mishima's study of the emulsified samples amorphized during cooling at high pressures and only moderately high cooling rates,[1] it was suggested that the glass transition of the high density amorphous phase has a large endothermic manifestation, *i.e.* that the ΔC_p is large, though the whole transition could not be well-observed because of crystallization. These observations and a parallel set on LiCl–H_2O solutions, led Mishima[1] to suggest "that the emulsified HDL is the solvent water of the high concentration electrolyte solution"; *i.e.* the water in aqueous solutions (*i.e.* "solvent water") was structurally related to HDL rather than to LDL. Our results, like those of the other solution $\Delta C_p(T_g)$ studies would tend to support such a conjecture.

However, this interesting idea must now be tempered by the recent direct measurements for large samples of high and low density amorphous water prepared and measured by Elsaesser *et al.*[53] These authors found that although the heat capacity change at T_g (which could be measured repeatedly without intervention of crystallization) was indeed larger for the HDA form, the difference was not by any means as large as is implied by the comparisons of LDA/LDL with the solution values that we have made earlier in this article. Thus we must recognize that, in both HDL (from VHDA), and LDL itself, the configurational restrictions on the liquid are much more severe, and the rate at which the changes in configuration can be excited by increase of temperature, much smaller, than can be achieved when the nearly completed networks of the pure water phases have been chemically disrupted by the presence of hydrating ions like Li^+ or alternate competitive hydrogen bonding sites offered by sugars, hydrazine molecules, or in the present case, phosphoric acid molecules and the derived anions.

How then, do we describe what is happening in the range where glasses no longer form?

The answer seems to lie in the observations of Mishima on lithium chloride that were referred to in the introduction. Mishima used pressure to widen the time scale separation between liquid state equilibration and crystallization, and this permitted him to observe, by refined thermal analysis studies, rather convincing evidence for a liquid–liquid phase separation. Coupled with the theoretical expectations of Chatterjee and Debenedetti[54] that such a phenomenon is to be expected when the solvent has a tendency to undergo a liquid–liquid polyamorphic transition, one concludes that the separating phase is the second (low temperature) phase of the polyamorphic transition of the pure solvent. In essence, the phase separation in the solution occurs because the solubility of the second (non-aqueous) component is much lower in the LDL phase of the solvent. Under these circumstances the homogeneous nucleation temperature reflects closely the phase boundary for the low temperature phase of water in the binary solution. As the ice nucleation slows down on approach to the glass transition the liquid–liquid phase transition becomes directly observable to the right sort of measurement.[3]

How general is this? Angell and Sare[4] studied the behavior of a large number of aqueous solutions at the end of their glassforming range, and found that they all seemed to have about the same limit when the glass temperature was plotted against equivalent rather than molar concentration. This implied that, near T_g, the cations of a given solution could reorient water molecules sufficiently to prevent them from joining the LDA structure, in proportion to their charge. Up to 30 H_2O per cation could be withheld in the case of trivalent cations, 21 for divalents, 11 for Li^+ and glasses generally did not form for the remaining alkali metal salts of simple anions. The number of waters restrained from crystallizing increases further with increase of pressure. The evidence from Mishima's study was that, near this limiting composition, the first step in the crystallization process was the separation into two liquids, one of them nearly pure LDL, after which the LDL would easily transform into ice Ic. The LDA phase, as in the case of liquid silicon, acts like a first Ostwald stage in the crystallization process.

Between the dilute solution, and the beginning of the fully glass-forming range, the addition of salt (and indeed many other second components) can be seen as increasing the stability of the HDA-like water component of the solution so that the solution resists crystallization down to lower temperatures, until the temperature reaches the solution T_g. Indeed, such a stabilization of the HDA-like water component

has been recorded in recent molecular dynamics studies of two component salt + water solutions.[55,56]

Two matters of interest arise in this case. The first concerns the size of the droplets of the new water phase that are trapped in the glassy state, and the second is the nature of the fluctuations that must occur in anticipation of the phase separation in the solution before it reaches the phase boundary.

A provocative answer to the first of these concerns was provided by the interesting simulation[57] of a solution of hydrophilic solute (modeling LiCl) in solution in the fast running water model known as mW water (monatomic water) because of its relation to the monoatomic liquid silicon from which the form of its intermolecular pair potential was taken.[58] The conclusion was that, although the liquid–liquid transition was unambiguous, the phase separation would be unable to proceed, even to mesoscopic dimensions, because of the rapid decrease in nucleation barrier as the size of the nanodomains increases. During coarsening, the crystallization rate would increase so that no macroscopic samples of LDA would become available by this route.

The second and more pervasive of the concerns involves the fluctuations that might be observed as the phase boundary is approached during cooling. Here we can now begin to understand the complexity of the aqueous solution structures that must be expected as we pass from the extended composition domain in which the T_g can be described by the CK model discussed earlier, and the state of pure water. In this composition range, especially as the solubility limit is approached, the fluctuations in composition and composition-dependent properties must grow rapidly. We can form some idea from the extensive literature on liquid–liquid separation in alkali silicate glasses, which we have argued elsewhere has the same polyamorphic origin as in aqueous systems.[59] In the case of alkali silicate glasses there have been intensive electron microscopy studies of the distribution of phases in the two phase domain.[60] Complex interconnecting patterns, which may be bicontinuous, form by the overlap of growing nucleation centers of the silica-rich phase, which is indeed nearly pure silica. We can expect that in the aqueous systems, a similar pattern would appear in the glassy domain near the edge of the glassforming range, while in the supercooled liquids above the phase boundary a similar but less well-defined and shorter-lived version of the same sort of wormhole structure might be obtained, as water molecules detach from hydration shells and join in LDL-like water clusters, and *vice versa*. The term "wormhole structure" has been used in the description of both aqueous solutions and alkali silicate glasses, though the qualifier, "transient", should be used for the liquid solution structure. It seems likely that, in a careful study of heat capacity near the edge of the glassforming range, where the liquid–liquid phase separation can be observed without interference from crystallization, the transition in heat capacity from the large value used in our CK model fitting of the T_g *vs.* composition function, towards the near-vanishing value of the pure water phase, would be observable directly.

6. Conclusions

The glass transition temperature of the P_2O_5–H_2O system has been measured using DSC over a wide range of compositions never explored before. In the range of concentration where comparisons are possible, our results are in rather good agreement with those determined recently using the same technique,[26] but they are lower than those measured by NMR.[23]

Special attention has been given to the determination of the T_g of pure orthophosphoric acid, which is a compound of great interest for which the values reported in the literature[22,24,25] differ by almost 80 K. The average T_g (onset) was (190 ± 3) K, which lies between the above mentioned values, and is close to the value T_g = 201 K, interpolated from the data by Aihara *et al.*[26]

The glass transition temperature could be described reasonably well all over the whole range of compositions by the Couchman and Karasz model.[5] The agreement between the best fit k parameter in eqn (5) and the theoretical value, obtained using the available data for the heat capacity change of P_2O_5 and water, is excellent, provided that we use ΔC_{p1} = 35 J K^{-1} mol^{-1}, the value extrapolated for water using data for solutions with other hydrogen bonding molecular solutes, and close to the value determined in this work by extrapolations of the heat capacity changes of the present H_3PO_4 (or P_2O_5) solutions.

This would support, and with some important modifications extend, the hypothesis by Mishima[1] that HDL is the solvent water of electrolyte solutions. In his case it was based on high pressure observations of ionic solutions whereas in the present case it is based on ambient pressure study of hydrogen bonding molecular solutions and thus acquires more general significance. The important point is that near the glass transition, solvent water, to a much greater extent that with any other molecular solvent in our experience, behaves quite differently than it does in its pure solvent state.

Acknowledgements

The authors thank financial support from Agencia Nacional de Promoción Científica y Tecnológica (PICT 06-32916), from Consejo Nacional de Investigaciones Científicas y Técnicas (CONICET, PIP 5977) and from University of Buenos Aires (Project X-050). The help of Dr Pilar Buera (Department of Industry, University of Buenos Aires) with the DSC measurements is gratefully acknowledged. HRC is a member of the CONICET. FNP thanks doctoral fellowships from CNEA and CONICET.

References

1 O. Mishima, *J. Chem. Phys.*, 2004, **121**, 3161.
2 O. Mishima, *J. Chem. Phys.*, 2005, **123**, 154506.
3 O. Mishima, *J. Chem. Phys.*, 2007, **126**, 244507.
4 C. A. Angell and E. J. Sare, *J. Chem. Phys.*, 1970, **52**, 1058.
5 P. R. Couchman and F. E. Karasz, *Macromolecules*, 1978, **11**, 117.
6 G. Adam and J. H. Gibbs, *J. Chem. Phys.*, 1965, **43**, 139.
7 J. E. Shelby, *Introduction to Glass Science and Technology*, Royal Society of Chemistry, 2nd edn, 2002.
8 R. T. Croswell, A. Reisman, D. L. Simpson, D. Temple and C. K. Williams, *J. Electrochem. Soc.*, 1999, **146**, 4569.
9 L. M. Sharaf El-Deen, M. S. Al Salhi and M. M. Elkholy, *J. Non-Cryst. Solids*, 2008, **354**, 3762.
10 J. W. Zwanziger, J. L. Shaw, U. Werner-Zwanziger and B. G. Aitken, *J. Phys. Chem. B*, 2006, **110**, 20123.

11 S. W. Martin and C. A. Angell, *J. Non-Cryst. Solids*, 1986, **83**, 185.
12 A. J. Parsons and C. D. Rudd, *J. Non-Cryst. Solids*, 2008, **354**, 4661.
13 L. A. Diaz, G. C. Abuin and H. R. Corti, *J. Power Sources*, 2009, **188**, 45.
14 W. L. Hill, G. T. Faust and S. B. Hendricks, *J. Am. Chem. Soc.*, 1943, **65**, 794.
15 D. E. C. Corbridge, *The Structural Chemistry of Phosphorus*, Elsevier Scientific Publishing Company, Amsterdam, 1974.
16 S. Sakka and J. D. McKenzie, *J. Non-Cryst. Solids*, 1971, **6**, 145.
17 R. L. Cormia, J. D. Mackenzie and D. J. Turnbull, *J. Appl. Phys.*, 1963, **34**, 2245.
18 S. W. Martin and C. A. Angell, *J. Phys. Chem.*, 1986, **90**, 6736.
19 J. J. Hudgens and S. W. Martin, *J. Am. Ceram. Soc.*, 1993, **76**, 1691.
20 D. L. Sidebottom and J. R. Changstrom, *Phys. Rev. B: Condens. Matter Mater. Phys.*, 2008, **77**, 020201R.
21 R. Böhmer, K. L. Ngai, C. A. Angell and D. J. Plazek, *J. Chem. Phys.*, 1993, **99**, 4201.
22 P. P. Kobeko, E. V. Kuvshinskii and N. J. Shishkin, *J. Phys. Chem. Mosc.*, 1937, **9**, 387.
23 B. Ellis, *Nature*, 1976, **263**, 674.
24 A. Eisenberg, H. Farb and L. G. Cool, *J. Polym. Sci., Part A-2*, 1966, **4**, 855.
25 A. D. F. Toy, *The Chemistry of Phosphorus*, Pergamon, Oxford, 1975, 482.
26 Y. Aihara, A. Sonai, M. Hattori and K. Hayamizu, *J. Phys. Chem. B*, 2006, **110**, 24999.
27 *Kirk–Othmer Encyclopedia of Chemical Technology*, John Wiley & Sons, 3rd edn, 1982, vol. 17, pp. 433.
28 M. Oguni and C. A. Angell, *J. Chem. Phys.*, 1980, **73**, 1948.
29 I. Kohl, L. Bachmann, E. Mayer, A. Hallbrucker and T. Loerting, *Nature*, 2005, **435**, E1.
30 M. H. Cohen and D. Turnbull, *J. Chem. Phys.*, 1959, **31**, 1164.
31 J. M Gordon and J. S. Taylor, *J. Appl. Chem.*, 1952, **2**, 493.
32 M. Goldstein, *Macromolecules*, 1985, **18**, 277.
33 P. R. Couchman, *Macromolecules*, 1987, **20**, 1712.
34 R. Pinal, *Entropy*, 2008, **10**, 207.
35 H. R. Corti, C. A. Angell, T. Auffret, H. Levine, M. P. Buera, D. S. Reid, Y. Roos and L. Slade, *Pure Appl. Chem.*, 2010, **82**, 1065.
36 G. Ten Brinkle, F. E. Karasz and T. S. Ellis, *Macromolecules*, 1983, **16**, 244.
37 M. Sugisaki, H. Suga and S. Seki, *Bull. Chem. Soc. Jpn.*, 1968, **41**, 2591.
38 A. Hallbrucker, E. Mayer and G. P. Johari, *J. Phys. Chem.*, 1989, **93**, 4986.
39 G. P. Johari, A. Hallbrucker and E. Mayer, *Science*, 1996, **273**, 90.
40 G. P. Johari, A. Hallbrucker and E. Mayer, *Nature*, 1987, **330**, 552.
41 A. Hallbrucker, E. Mayer and G. P. Johari, *Philos. Mag. B*, 1989, **60**, 170.
42 G. P. Johari, G. Astl and E. Mayer, *J. Chem. Phys.*, 1990, **92**, 809.
43 G. P. Johari, A. Hallbrucker and E. Mayer, *J. Chem. Phys.*, 1990, **92**, 6742.
44 I. Kohl, A. Hallbrucker and E. Mayer, *Phys. Chem. Chem. Phys.*, 2000, **2**, 1579.
45 D. R. MacFarlane and C. A. Angell, *J. Phys. Chem.*, 1984, **88**, 759.
46 C. A. Angell and J. C. Tucker, *J. Phys. Chem.*, 1980, **84**, 268.
47 K. Ito, C. T. Moynihan and C. A. Angell, *Nature*, 1999, **398**, 492.
48 C. A. Angell, *Science*, 2008, **319**, 582.
49 Y. Yue and C. A. Angell, *Nature*, 2004, **427**, 717.
50 O. Mishima, *Nature*, 1996, **384**, 546.
51 R. J. Nelmes, J. S. Loveday, T. Straessle, C. L. Bull, M. Guthrie, G. Hamel and S. Klotz, *Nat. Phys.*, 2006, **2**, 414.
52 T. Loerting, K. Winkel, M. Seidl, M. Bauer, C. Mitterdorfer, P. H. Handle, C. G. Salzmann, E. Mayer, J. L. Finney and D. T. Bowron, *Phys. Chem. Chem. Phys.*, 2011, **13**, 8783.
53 M. S. Elsaesser, K. Winkel, E. Mayer and T. Loerting, *Phys. Chem. Chem. Phys.*, 2010, **12**, 708.
54 S. Chatterjee and P. G. Debenedetti, *J. Chem. Phys.*, 2006, **124**, 154503.
55 D. Corradini, M. Rovere and P. Gallo, *J. Phys. Chem. B*, 2011, **115**, 1461.
56 M. P. Longinotti, M. A. Carignano, I. Szleifer and H. R. Corti, *J. Chem. Phys.*, 2011, **134**, 244510.
57 E. B. Moore and V. Molinero, *J. Chem. Phys.*, 2010, **132**, 244504.
58 V. Molinero and E. B. Moore, *J. Phys. Chem. B*, 2009, **113**, 4008.
59 C. A. Angell, P. H. Poole and M. Hemmati, *Proc. 12th East European Glass Conf.*, ed. B. Samunova and Y. Demetriew, Varna, Bulgaria, 1998, pp. 100–109.
60 W. Haller and P. B. Macedo, *Phys. Chem. Glasses*, 1968, **9**, 153.

